

# The rotation state of 67P/Churyumov-Gerasimenko from approach observations with the OSIRIS cameras on Rosetta<sup>★</sup>

S. Mottola<sup>1</sup>, S. Lowry<sup>2</sup>, C. Snodgrass<sup>3</sup>, P. L. Lamy<sup>4</sup>, I. Toth<sup>5</sup>, A. Rožek<sup>2</sup>, H. Sierks<sup>3</sup>, M. F. A'Hearn<sup>6</sup>, F. Angrilli<sup>7</sup>, C. Barbieri<sup>7</sup>, M. A. Barucci<sup>8</sup>, J.-L. Bertaux<sup>9</sup>, G. Cremonese<sup>10</sup>, V. Da Deppo<sup>11</sup>, B. Davidsson<sup>12</sup>, M. De Cecco<sup>13</sup>, S. Debei<sup>14</sup>, S. Fornasier<sup>8</sup>, M. Fulle<sup>15</sup>, O. Groussin<sup>4</sup>, P. Gutiérrez<sup>16</sup>, S. F. Hviid<sup>1</sup>, W. Ip<sup>17</sup>, L. Jorda<sup>4</sup>, H. U. Keller<sup>18</sup>, J. Knollenberg<sup>1</sup>, D. Koschny<sup>19</sup>, R. Kramm<sup>3</sup>, E. Kührt<sup>1</sup>, M. Küppers<sup>20</sup>, L. Lara<sup>16</sup>, M. Lazzarin<sup>7</sup>, J. J. Lopez Moreno<sup>16</sup>, F. Marzari<sup>21</sup>, H. Michalik<sup>22</sup>, G. Naletto<sup>23</sup>, H. Rickman<sup>12</sup>, R. Rodrigo<sup>24,25</sup>, L. Sabau<sup>26</sup>, N. Thomas<sup>27</sup>, K-P Wenzel<sup>19</sup>, J. Agarwal<sup>3</sup>, I. Bertini<sup>28</sup>, F. Ferri<sup>28</sup>, C. Güttler<sup>3</sup>, S. Magrin<sup>6</sup>, N. Oklay<sup>3</sup>, C. Tubiana<sup>3</sup>, J.-B. Vincent<sup>3</sup>

(Affiliations can be found after the references)

Received 11 July 2014, XXXX; accepted XXX, XXXX

## ABSTRACT

**Aims.** Approach observations with the OSIRIS experiment onboard Rosetta are used to determine the rotation period, the direction of the spin axis and the state of rotation of comet 67P's nucleus.

**Methods.** Photometric time series of 67P have been acquired by OSIRIS since the post wake-up commissioning of the payload in March 2014. Fourier analysis and convex shape inversion methods have been applied to the Rosetta data as well to the available ground-based observations.

**Results.** Evidence is found that the rotation rate of 67P has significantly changed near the time of its 2009 perihelion passage, probably due to sublimation-induced torque. We find that the sidereal rotation periods  $P_1 = 12.76129 \pm 0.00005$  h and  $P_2 = 12.4043 \pm 0.0007$  h for the apparitions before and after the 2009 perihelion, respectively, provide the best fit to the observations. No signs of multiple periodicity are found in the lightcurves down to the noise level, which implies that the comet is presently in a simple rotation state around its axis of largest moment of inertia. We derive a prograde rotation model with spin vector J2000 ecliptic coordinates  $\lambda = 65^\circ \pm 15^\circ$ ,  $\beta = +59^\circ \pm 15^\circ$  (corresponding to equatorial coordinates  $RA = 22^\circ$ ,  $Dec = +76^\circ$ ). However, we find that the mirror solution, also prograde, at  $\lambda = 275^\circ \pm 15^\circ$ ,  $\beta = +50^\circ \pm 15^\circ$  (or  $RA = 274^\circ$ ,  $Dec = +27^\circ$ ) is also possible at the same confidence level, due to the intrinsic ambiguity of the photometric problem for observations performed close to the ecliptic plane.

**Key words.** comets: general – comets: individual: 67P/Churyumov-Gerasimenko – techniques: photometric

## 1. Introduction

Following the Rosetta wake-up after hibernation and subsequent recommissioning of the scientific payload, which occurred in March 2014, OSIRIS, the main imaging system onboard the ESA spacecraft, started performing periodic photometric observations of the target comet 67P/Churyumov-Gerasimenko (67P) from a range of about 5 million km. The goal of these approach observations is threefold: 1) to support the navigation of the spacecraft through optical imaging; 2) to perform early characterization of the comet in order to determine its rotational state and 3) to monitor the onset of cometary activity. The last two points, besides their own scientific interest, provide valuable input for the planning of the mission operations at the comet. Comet 67P was selected as a Rosetta target only after a delay in the Ariane launcher program made it impossible for the mission to reach its originally scheduled target, comet 46P/Wirtanen. At that time, however, and only two orbital revolutions around the Sun before the scheduled Rosetta encounter, important physical properties of 67P, as its rotation state, were still unknown. Early work by Lamy et al. (2006) based on HST observations, provided a first determination of the rotation state of the comet, indicating a simple rotation and a period in the range 12.0 h to 12.8 h. The authors also performed photometric inversion of

the HST lightcurve, which resulted in a non-convex, and admittedly non-unique, shape model. Further lightcurve observations were performed by Lowry et al. (2006) and by Tubiana et al. (2008, 2011). Lowry et al. (2012) used all the observational base available at that time, and derived a best spin state solution with  $P_{sid} = 12.76137 \pm 0.00006$  h and ecliptic coordinates of the pole  $\lambda = 78^\circ \pm 10^\circ$ ;  $\beta = +58^\circ \pm 10^\circ$ , along with a convex shape model.

## 2. Observations and data reduction

The results presented in this paper are based on observations performed with the OSIRIS instrument (Keller et al. 2007) in 2014 in the period Mar 23 to Jun 24 (see Table 1 in the Online Material for the observational circumstances). OSIRIS consists of a suite of two cameras, the NAC (Narrow Angle Camera) and the WAC (Wide Angle Camera). They both use a  $2048 \times 2048$  pixel CCD camera coupled to a reflective telescope – an f/8 telescope with a  $2.2^\circ \times 2.2^\circ$  field of view (FOV) for the NAC and an f/5.6,  $11.3^\circ \times 12.1^\circ$  FOV telescope for the WAC. The images used for this study were acquired with the NAC filter 22 (center band 649.2 nm, FWHM 84.5 nm) and WAC filter 12 (center band 629.8 nm, FWHM 156.8 nm). Typical exposure times ranged from 10 s to 12 min, selected to achieve the maximum possible signal to noise ratio (SNR) at the different ranges from the comet and still avoid saturation. High SNR was necessary for

<sup>★</sup> Table 1 is only available in electronic form at <http://www.aanda.org/>

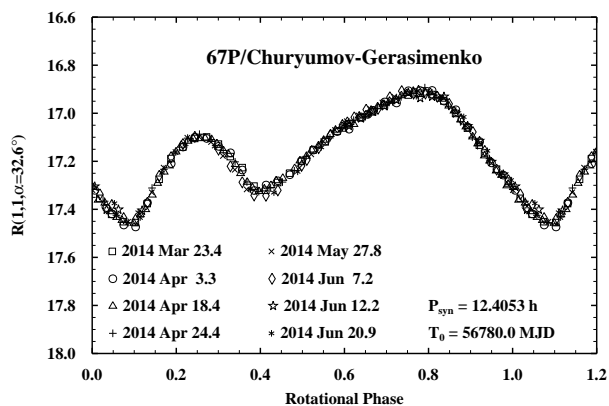


**Fig. 1.** Composite lightcurve from the OSIRIS observations. The nuclear magnitudes are reduced to the standard observation geometry at 1 AU. The magnitude scale refers to the phase angle at the time of the first NAC observations. The following observations have been accordingly shifted in magnitude. Data points beyond rotational phase 1.0 are repeated for clarity.  $T_0$  is corrected for light-travel time. The dates refer to the mid-time of the respective observation.

imaging the faint coma and for the detection of possible subtle deviations from strict periodicity in the lightcurves. Depending on whether the images were acquired for navigation purposes or for lightcurve studies, the data were either relayed as full frames to Earth or as small subframes centered around the target, as a measure for limiting data volume. The raw frames were pre-processed through the standard OSIRIS data reduction pipeline while the comet fluxes were measured with the AstPhot synthetic aperture photometry tool (Mottola et al. 1995). The raw fluxes were then reduced to the standard observation geometry at 1 AU from the observer and from the Sun, and then converted to the Kron-Cousins R band by using OSIRIS standard calibration fields. No correction for changing phase angle was applied. The typical relative photometric error of the measurements is about 0.01 mag ( $1-\sigma$ ), while the systematic absolute photometric calibration error is estimated to be of the order of 0.03 mag. During the observation period the nucleus was still unresolved on both cameras, and the comet experienced episodes of intermittent activity (Tubiana et al, in prep.) which resulted in the presence of a clearly visible coma in some of the acquisition sessions. In order to minimize the coma contribution to the measured nuclear magnitude we selected a small circular synthetic aperture with a radius of 4 pixels. At the distance of the comet this aperture size corresponded to a projected radius of 50 km for the single WAC observation, while it ranged from 272 km to 15 km for the NAC observations. No attempt was made to model and subtract the coma contribution to the lightcurves, as it was estimated to be smaller than the relative photometric error of the measurements. In order to determine the rotation period, the OSIRIS photometric time series were analyzed with the Fourier analysis procedure described in Harris et al. (1989). In this method, a light curve is approximated with a Fourier polynomial of the desired order. For each trial rotation period within a given range, a linear equation system is constructed, which is then least-squares fitted to the data to retrieve the best-fit Fourier coefficients and the magnitude offset for each individual night. A solution is achieved if a global minimum of the residuals in the chi-squared sense is found. The resulting composite lightcurve is shown in Fig. 1. The best-fit period is  $12.4053 \pm 0.0007$  h, with an amplitude of  $0.542 \pm 0.005$  mag. Although this period strictly represents a synodic period, the direction of the phase angle bisector (PAB, see Harris et al. (1984) for a definition) changed only by about  $7^\circ$  during the three

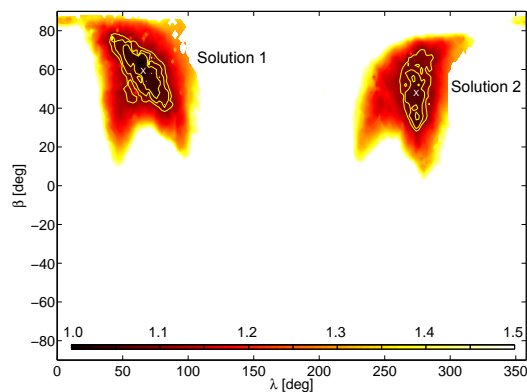


**Fig. 2.** Normalized  $\chi^2$  map showing the goodness of the fit to the lightcurves as a function of the ecliptic coordinates of the spin axis. The contour lines show the +5%, +7.5% and +10% levels from the minimum  $\chi^2$ .

months spanned by the OSIRIS observations. For this reason, the measured comet's synodic period is very close to the sidereal one.

### 3. Rotation state

The composite in Fig. 1 shows that the 67P lightcurves nicely overlap at the level of the photometric noise. No multiple periodicities are detected, which demonstrates that the comet is presently in (or very close to) a relaxed rotation state. Soon after the first few OSIRIS lightcurves were acquired, it became apparent that the measured rotation period significantly differed from the best solution from Lowry et al. (2012). Unfortunately, the HST observations of 2003 by Lamy et al. (2006), given their short time baseline, are compatible with either period, and don't allow discriminating among them. Intriguingly enough, a possible solution with a period of about 12.4 h was found by Lowry et al. (2012) during their initial period scan (cfr. their Fig. 2). This solution, however, was disregarded by the authors as unreliable, as it caused some of the lightcurves to appear in counter-phase in the composite.

As a first step for the determination of the spin state of 67P we searched for a global period-pole-shape solution by using the convex shape inversion scheme (Kaasalainen et al. 2001; Kaasalainen & Torppa 2001) on the complete data set available (see Table 1). Solutions were found around a period of 12.4 h which produced satisfactory fits to the lightcurves in terms of  $\chi^2$  and general lightcurve shapes. However, the family of convex shape models corresponding to those solutions all consisted of a pure rotation around the long-axis of the body (long-axis mode – LAM). Pure LAM rotation corresponds to the maximum allowable energetic state for a given angular momentum of the body. Therefore we consider it unlikely that 67P can presently occupy exactly this energy state. Other (non pure) LAM states have been observed (or proposed) for several comets and asteroids as 1P/Halley and (4179) Toutatis. They represent excited rotation states which are always associated with precession of the instantaneous spin vector of the body (see e.g. Samarasinha & A'Hearn 1991). Such complex rotation, however, would necessarily cause a typical signature in the lightcurves, which was definitely not present in the OSIRIS observations.

Given that no viable single solution was found which could satisfy all of the available photometric observations, we considered the possibility that the rotation period of 67P could have evolved with time, subjected to a sublimation-induced torque.

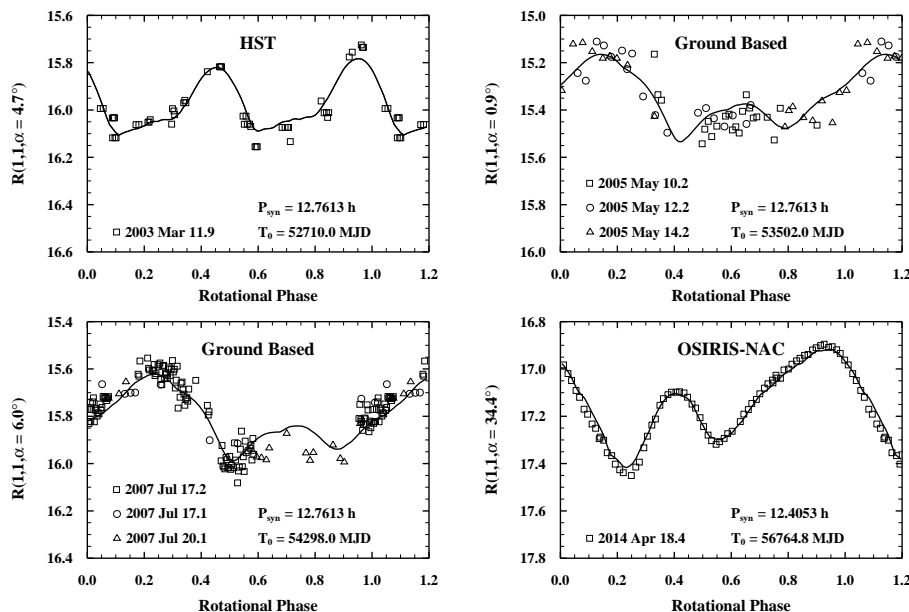


**Fig. 3.** HST, ground-based and OSIRIS NAC selected lightcurves of 67P (from top left to bottom right) along with synthetic curves obtained with the shape model corresponding to Solution 1 (solid line). See Table 1 for observational details.

This choice was encouraged by the fact that both modeling and observations are providing increasing evidence that a spin period may change during a single orbital step. The last perihelion passage of 67P occurred on Feb 28, 2009, and the previous one on Sep 18, 2002. Therefore, all pre-Rosetta observations were obtained in the time interval between the past two perihelion passages, while the OSIRIS observations were performed after the 2009 perihelion. We therefore made the working hypothesis that the spin rate of 67P changed during some period around the perihelion of 2009 (due to cometary activity), while staying constant during the two time intervals covered by the ground-based and Rosetta observations, respectively. We consequently modified the convex inversion procedure to allow for two independent rotation periods, one before and one after the 2009 perihelion passage. The second period was kept fixed at the value found through the OSIRIS observations, which provided a very solid constraint, while the first period was left free as an optimization parameter.

Figure 2 represents a plot of the normalized  $\chi^2$  of the fit as a function of the ecliptic coordinates of the pole. Two regions with significantly lower residuals than the background are clearly identifiable in the plot and are labeled as Solution 1 and Solution 2. These regions are centered around J2000 ecliptic coordinates ( $\lambda = 65^\circ$ ;  $\beta = +59^\circ$ ) and ( $\lambda = 275^\circ$ ;  $\beta = +50^\circ$ ), respectively, and are both characterized by the same set of sidereal periods ( $P_1 = 12.76129 \pm 0.00005$ ;  $P_2 = 12.4043 \pm 0.0007$ ). Because the loci of the solutions have an irregular shape, simple errors on the coordinates do not well represent the accuracy of the pole location. Having this limitation in mind, we estimate the uncertainty in the orientation of the spin axis to be on the order of  $\pm 15^\circ$  for each ecliptic coordinate, and refer the reader to Fig. 2 for a more realistic representation. The two solutions, however, are not independent, and are a manifestation of the ambiguity theorem as formulated by Kaasalainen & Lamberg (2006). This theorem states that if the viewing and illumination geometry (i.e. the Sun and observer vectors) lie on the same plane for all observations (usually the ecliptic), and if  $(\lambda, \beta)$  constitutes a solution that satisfies the lightcurves, then also  $(\lambda + 180^\circ, \beta)$  represents a solution for a model shape which is a mirror along the z-axis

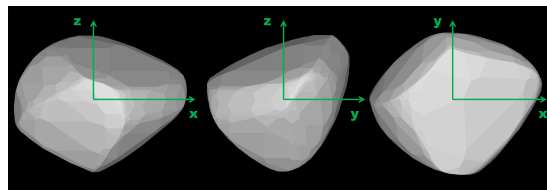


**Fig. 4.** Three orthogonal views of the convex shape model corresponding to Solution 1.

of the shape model for the original solution. Since 67P has a small orbital inclination, indeed the viewing geometry was close to (but not exactly on) the ecliptic plane for all the observations, which resulted in the observed ambiguity. This small deviation from the ecliptic geometry causes the two conjugate solutions not to be spaced by exactly  $180^\circ$  in ecliptic longitude. Our Solution 1 is compatible with the less favorite prograde solution by Lamy et al. (2007) and with the most likely solution by Lowry et al. (2012).

Figure 3 shows the model fits to selected lightcurves corresponding to the Solution 1. It can be seen that the model provides an excellent fit to the observations both in terms of phasing of the lightcurve features, and in terms of amplitude. Solution 2 results in a similarly good fit. Figure 4 shows the corresponding convex shape model in three orthogonal views. It must be emphasized that the obtained shape represents the best "photometric" shape. Kaasalainen & Torppa (2001) have demonstrated that their inversion scheme converges to the real shape of the object if the object is globally convex. If the object, on the other hand, contains major concavities, the inversion procedure converges to the convex hull of the body – the shape that a non-convex body would have if it was "shrink-wrapped". The occurrence of several large planar facets on our shape model is therefore a hint that major concavities might be present at those locations.

#### 4. Discussion and conclusions

With axial ratios of  $a/b = 1.21$  and  $b/c = 1.05$ , the derived shape is less elongated than the one found by Lowry et al. (2012), with

the uncertainty being largest on the z-axis dimension due to the view near the ecliptic plane for all data sets. The presence of large flat faces (or depressions) on the surface is seen in both models.

The change in rotation rate – with the period shortening by around 21 minutes over the course of the 2009 perihelion passage – is within the expected range for comets. Gutiérrez et al. (2005), for example, estimated for 67P a possible change of period between orbits could be up to one hour. Four previous determinations of period changes in short period comets have been made, with magnitudes between 16 seconds per orbit for the low activity comet 10P/Tempel 2 (Knight et al. 2012) and 2 hours for the hyperactive 103P/Hartley 2 (Belton et al. 2013). The other measurements were for 2P/Encke (4 minutes – Mueller et al. (2008)) and 9P/Tempel 1 (14 minutes – Belton et al. (2011); Chesley et al. (2013)). It is not surprising that the change for 67P is similar to that for 9P, a comet of similar size and activity level, although with a considerably longer rotation period (41 h). Samarasinha & Mueller (2013) compared the four comets with observed spin-rate changes and their activity level, and found that an approximately constant factor (within a factor of two) links them and allows the change of rotation rate to be predicted based on the size, period and orbit of the comet, and that the changes should be independent of the active fraction of the surface area. The measurement for 67P is 2-3 times larger than this analysis predicted (Samarasinha, private communication).

A more detailed analysis of how and when the period changed is beyond the scope of this short letter, and will include further constraints from ground-based observation. As the comet's activity is largely similar from orbit to orbit (Snodgrass et al. 2013), and 9P was seen to have a similar change in period each perihelion (Belton et al. 2011), we can expect that the comet's period will decrease by a further ~20 minutes during the coming perihelion passage. With the high precision on  $\Delta P$  possible by landmark tracking from OSIRIS images, a change of this magnitude will be easy to detect, and furthermore the rate of change as the comet approaches the Sun will be determined, giving us information on the moment of inertia and torques due to outgassing at different times.

**Note:** Resolved images of 67P from OSIRIS have subsequently found a highly irregular shape, and a rotation pole consistent with Solution 1. Details on the shape from resolved images, and a comparison with the convex hull solution presented here, will be presented at a later date.

*Acknowledgements.* OSIRIS was built by a consortium of the Max-Planck-Institut für Sonnensystemforschung, in Göttingen, Germany, CISAS–University of Padova, Italy, the Laboratoire d'Astrophysique de Marseille, France, the Instituto de Astrofísica de Andalucía, CSIC, Granada, Spain, the Research and Scientific Support Department of the European Space Agency, Noordwijk, The Netherlands, the Instituto Nacional de Técnica Aeroespacial, Madrid, Spain, the Universidad Politécnica de Madrid, Spain, the Department of Physics and Astronomy of Uppsala University, Sweden, and the Institut für Datentechnik und Kommunikationsnetze der Technischen Universität Braunschweig, Germany. The support of the national funding agencies of Germany (DLR), France (CNES), Italy (ASI), Spain (MEC), Sweden (SNSB), and the ESA Technical Directorate is gratefully acknowledged. CS received funding from the European Union Seventh Framework Programme (FP7/2007-2013) under grant agreement no. 268421. This research made use of JPL's online ephemeris generator HORIZONS.

## References

Belton, M. J. S., Meech, K. J., Chesley, S., et al. 2011, *Icarus*, 213, 345  
 Belton, M. J. S., Thomas, P., Li, J.-Y., et al. 2013, *Icarus*, 222, 595  
 Chesley, S. R., Belton, M. J. S., Carcich, B., et al. 2013, *Icarus*, 222, 516  
 Gutiérrez, P. J., Jorda, L., Samarasinha, N. H., & Lamy, P. 2005, *Planet. Space Sci.*, 53, 1135

Harris, A. W., Young, J. W., Bowell, E., et al. 1989, *Icarus*, 77, 171  
 Harris, A. W., Young, J. W., Scaltriti, F., & Zappala, V. 1984, *Icarus*, 57, 251  
 Kaasalainen, M. & Lamberg, L. 2006, *Inverse Problems*, 22, 749  
 Kaasalainen, M. & Torppa, J. 2001, *Icarus*, 153, 24  
 Kaasalainen, M., Torppa, J., & Muinonen, K. 2001, *Icarus*, 153, 37  
 Keller, H. U., Barbieri, C., Lamy, P., et al. 2007, *Space Sci. Rev.*, 128, 433  
 Knight, M. M., Schleicher, D. G., Farnham, T. L., Schwieterman, E. W., & Christensen, S. R. 2012, *AJ*, 144, 153  
 Lamy, P. L., Toth, I., Davidsson, B. J. R., et al. 2007, *Space Sci. Rev.*, 128, 23  
 Lamy, P. L., Toth, I., Weaver, H. A., et al. 2006, *A&A*, 458, 669  
 Lowry, S., Duddy, S. R., Rozitis, B., et al. 2012, *A&A*, 548, A12  
 Lowry, S. C., Fitzsimmons, A., Jorda, L., et al. 2006, in *BAAS*, Vol. 38, AAS/Division for Planetary Sciences Meeting Abstracts #38, 492  
 Mottola, S., De Angelis, G., Di Martino, M., et al. 1995, *Icarus*, 117, 62  
 Mueller, B. E. A., Samarasinha, N. H., & Fernandez, Y. R. 2008, in *Bulletin of the American Astronomical Society*, Vol. 40, AAS/Division for Planetary Sciences Meeting Abstracts #40, 416  
 Samarasinha, N. H. & A'Hearn, M. F. 1991, *Icarus*, 93, 194  
 Samarasinha, N. H. & Mueller, B. E. A. 2013, *ApJ*, 775, L10  
 Snodgrass, C., Tubiana, C., Bramich, D. M., et al. 2013, *A&A*, 557, A33  
 Tubiana, C., Barrera, L., Drahus, M., & Boehnhardt, H. 2008, *A&A*, 490, 377  
 Tubiana, C., Bönhardt, H., Agarwal, J., et al. 2011, *A&A*, 527, A113

- 1 Institute of Planetary Research, DLR, Rutherfordstrasse 2, 12489 Berlin, Germany; e-mail: stefano.mottola@dlr.de
- 2 Centre for Astrophysics and Planetary Science, School of Physical Sciences, The University of Kent, Canterbury, CT2 7NH, UK
- 3 Max-Planck-Institut für Sonnensystemforschung, Justus-von-Liebig-Weg, 3 37077 Göttingen, Germany
- 4 Aix Marseille Université, CNRS, LAM (Laboratoire d'Astrophysique de Marseille) UMR 7326, 13388, Marseille, France
- 5 Konkoly Observatory, MTA CSFK CSI, Budapest, PO Box H-1525, Hungary
- 6 Department for Astronomy, University of Maryland, College Park, MD 20742-2421, USA
- 7 University of Padova, Department of Physics and Astronomy, vicolo dell'Osservatorio 3, 35122, Padova, Italy
- 8 LESIA, Obs. de Paris, CNRS, Univ Paris 06, Univ. Paris-Diderot, 5 Place J. Janssen, 92195 Meudon, France
- 9 LATMOS, CNRS/UVSQ/IPSL, 11 Boulevard d'Alembert, 78280 Guyancourt, France
- 10 INAF–Osservatorio Astronomico di Padova, Vicolo dell'Osservatorio 5, 35122 Padova, Italy
- 11 CNR–IFN UOS Padova LUXOR, Via Trasea 7, 35131 Padova, Italy
- 12 Department of Physics and Astronomy, Uppsala University, 75120 Uppsala, Sweden
- 13 UNITN, Università di Trento, Via Mesiano, 77, 38100 Trento, Italy
- 14 Department of Mechanical Engineering – University of Padova, Via Venezia 1, 35131 Padova, Italy
- 15 INAF – Osservatorio Astronomico di Trieste, via Tiepolo 11, 34143 Trieste, Italy
- 16 Instituto de Astrofísica de Andalucía – CSIC, 18080 Granada, Spain
- 17 Institute for Space Science, National Central University, 32054 Chung-Li, Taiwan
- 18 Institute for Geophysics and Extraterrestrial Physics, TU Braunschweig, 38106 Braunschweig, Germany
- 19 Research and Scientific Support Department, European Space Agency, 2201 Noordwijk, The Netherlands
- 20 ESA/ESAC, PO Box 78, 28691 Villanueva de la Cañada, Spain
- 21 Dept. Physics, University of Padova, Italy
- 22 Institut für Datentechnik und Kommunikationsnetze, 38106 Braunschweig, Germany
- 23 Department of Information Engineering - University of Padova, Via Gradenigo 6, 35131 Padova, Italy
- 24 Centro de Astrobiología (INTA-CSIC), Spain
- 25 International Space Science Institute, Switzerland
- 26 Instituto Nacional de Técnica Aeroespacial, 28850 Torrejón de Ardoz, Spain
- 27 Physikalisches Institut, Sidlerstrasse 5, University of Bern, CH-3012 Bern, Switzerland
- 28 University of Padova, CISAS, via Venezia 15, 35100 Padova, Italy

**Table 1.** Observational circumstances

Date (UT)	PAB (J2000)			r (AU)	$\Delta$ (AU)	Instrument	References
	$\lambda$ ( $^{\circ}$ )	$\beta$ ( $^{\circ}$ )	$\alpha$ ( $^{\circ}$ )				
2003 Mar 11.9	165.9	+8.5	4.7	2.5033	1.5231	HST	Lamy et al. (2006)
2005 May 10.2	233.8	-0.3	0.9	5.5994	4.5923	NTT	Lowry et al. (2012)
2005 May 12.2	233.6	-0.3	0.5	5.6017	4.5921	NTT	Lowry et al. (2012)
2005 May 14.2	233.5	-0.4	0.1	5.6039	4.5932	NTT	Lowry et al. (2012)
2006 May 26.2	250.7	-2.6	1.3	5.6199	4.6134	VLT	Tubiana et al. (2008)
2006 May 31.2	250.4	-2.6	0.6	5.6145	4.6019	VLT	Tubiana et al. (2008)
2006 Jun 01.2	250.3	-2.6	0.5	5.6135	4.6005	VLT	Tubiana et al. (2008)
2007 Jul 17.1	269.0	-5.3	6.0	4.6347	3.7168	NTT	Lowry et al. (2012)
2007 Jul 17.2	269.0	-5.3	6.0	4.6347	3.7168	VLT	Tubiana et al. (2008)
2007 Jul 20.1	268.8	-5.3	6.7	4.6234	3.7289	NTT	Lowry et al. (2012)
2014 Mar 23.4	263.1	+1.8	32.6	4.2866	0.0330	NAC	This work
2014 Apr 03.3	263.5	+1.7	33.4	4.2376	0.0280	NAC	This work
2014 Apr 18.4	264.2	+1.6	34.4	4.1696	0.0214	NAC	This work
2014 Apr 24.4	264.5	+1.6	34.8	4.1398	0.0186	NAC	This work
2014 May 27.8	266.8	+0.8	35.3	3.9772	0.0048	NAC	This work
2014 Jun 07.2	268.1	+0.2	34.3	3.9248	0.0024	NAC	This work
2014 Jun 12.2	268.6	+0.0	34.1	3.8980	0.0018	NAC	This work
2014 Jun 20.9	270.0	-0.4	32.7	3.8533	0.0010	WAC	This work

**Notes.** The date refers to the UT of the mid-time of the respective series of observations.  $\lambda$  and  $\beta$  are the ecliptic J2000 coordinates of the PAB.  $\alpha$  is the solar phase angle (Sun-Target-Observer).  $r$  and  $\Delta$  are the heliocentric and observer ranges of 67P, respectively. HST = Hubble Space Telescope; NTT = New Technology Telescope, La Silla, Chile; VLT = Very Large Telescope, Paranal, Chile; NAC = OSIRIS Narrow Angle Camera; WAC = OSIRIS Wide Angle Camera.